ACS OMEGA

http://pubs.acs.org/journal/acsodf

Article

Bioinspired Ion Pairs Transforming Papaverine into a Protic Ionic Liquid and Salts

Paul Güntzel, Klaus Schilling, Simon Hanio, Jonas Schlauersbach, Curd Schollmayer, Lorenz Meinel, and Ulrike Holzgrabe*

Cite This: *ACS Omega* 2020, 5, 19202−19209

Read Online

ACCESS | Metrics & More | Article Recommendations

ABSTRACT: Microbial, mammalian, and plant cells produce and contain secondary metabolites, which typically are soluble in water to prevent cell damage by crystallization. The formation of ion pairs, for example, with carboxylic acids or mineral acids, is a natural blueprint to maintain basic metabolites in solution. Here, we aim at showing whether the mostly large carboxylates form soluble protic ionic liquids (PILs) with the basic natural product papaverine resulting in enhanced aqueous solubility. The obtained PILs were characterized by $^{1}H-^{15}N$ HMBC nuclear magnetic resonance (NMR) and in the solid state using X-ray powder diffraction, differential scanning calorimetry, and dissolution measurements. Furthermore, their supramolecular pattern in aqueous solution was studied by means of potentiometric and photometrical solubility, NMR aggregation assay, dynamic light scattering, zeta potential, and viscosity measurements. Thereby, we identified the naturally occurring carboxylic acids, citric acid, malic acid, and tartaric acid, as being appropriate counterions for papaverine and which will facilitate the formation of PILs with their beneficial characteristics, like the improved dissolution rate and enhanced apparent solubility.

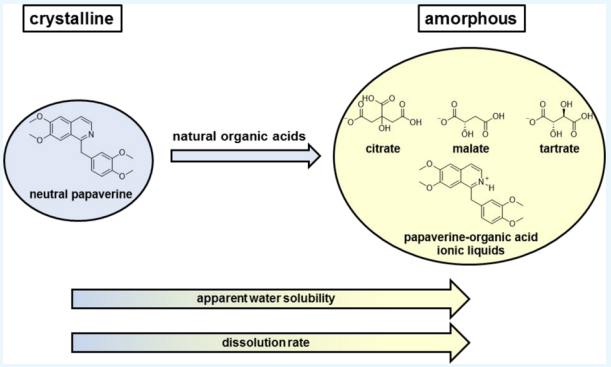

INTRODUCTION

Plant vacuoles are storage compartments for secondary metabolites such as alkaloids and flavonoids, as well as for small molecules like carboxylic acids, amino acids, and sugars. These organic acids may have higher concentrations in the vacuole than in the cytosol, whereas for most amino acids, the vacuolar concentrations were similar to the cytosolic concentrations.[1,2] Some carboxylates such as citrate and malate enter the vacuole by specific transporter proteins; they represent the major carboxylic acids in plants and play a major role in cellular processes and are involved in several metabolic pathways as intermediates of energy metabolism. Additionally, they may also serve as counterions for cationic alkaloids to improve their water solubility.[3,4] An early indicator of the importance of organic acid salts in nature was given by Sertürner in the 19th century. He isolated morphine as its meconate salt from opium, the dried milky sap from *Papaver somniferum*.[5,6]

Salt formation of poorly water-soluble organic bases with acids may increase apparent solubility in an aqueous environment compared to the free bases. The concept of salt formation is one among other pharmaceutical strategies, like cocrystal formation, complexation, and particle size reduction, to deal with the problem of poor water solubility and a low oral bioavailability of active pharmaceutical ingredients (APIs).[7] However, these salt formulations may suffer from poor solution stability within supersaturated states leading to API precipitation and hence improper adsorption from the gastrointestinal tract. Therefore, a constant high counterion-to-API ratio is necessary to prevent precipitation of the API, which leads to an increased duration of supersaturation and consequently to a more stable solution. A strategy combining salt formation and a reduction of the interaction between molecules, hence decrease of the melting point (mp), which may result in improved dissolution rates, is the formulation of an ionic liquid (IL).[8,9] ILs are defined as organic salts with mp's below 100 °C, with attractive properties, including low volatility, low flammability, polarity, and high viscosity.[9−12] They can be subdivided in protic ILs (PILs) and aprotic ILs (AILs). Many AILs have been prepared and characterized to date; most of them were based on halogenated counter anions

Received: June 3, 2020
Accepted: July 8, 2020
Published: July 22, 2020

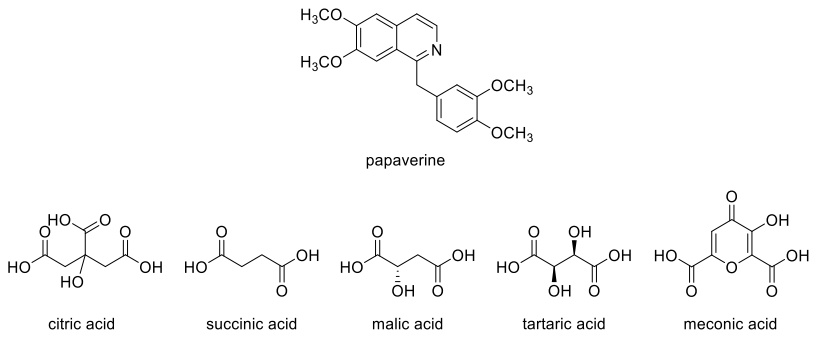

Figure 1. Used naturally occurring molecules.

such as tetrafluoroborate (BF_4^-), hexafluorophosphate (PF_6^-), and derivatives thereof. Because of toxicological and ecological issues, these halide-containing anions are not suitable for therapeutic applications. An alternative approach to overcome these drawbacks is the development of bioinspired ILs, which are solely composed of naturally occurring molecules—components having well characterized biodegradable and toxicological properties.[13] Larger counterions reduce lattice forces within crystals, which is why bulky natural carboxylic acids might be particularly valuable for PIL formation of basic, poorly water-soluble APIs with the ultimate goal of improved apparent solubility and/or dissolution rates.[14−16] PILs are prepared in a simple neutralization reaction of certain Brønsted acids and Brønsted bases in an equimolar ratio.[17,18] A subset of PILs is the protic oligomeric ILs (OILs), which are the result of a reaction of several equivalents of a Brønsted acid with one equivalent of a Brønsted base to form H-bonded acid oligomer-based ILs.[19,20]

The effect of organic acids or other dispersants with low molecular weight is mainly based on the charging of the surface of the powder particles, thereby increasing the repulsive double-layer forces. In the Derjaguin−Landau−Verwey−Overbeek (DLVO) theory, suspension's properties are determined by its attractive and repulsive forces. Attractive van der Waals forces can be counteracted by repulsive forces resulting from either overlapping of the electrical double layers ("electrostatic" stabilization) and/or layering of materials adsorbed on the surface ("steric" stabilization).[21,22]

Considering numerous beneficial properties of liquid salts, including improved water solubility and dissolution rate, ILs have drawn the attention of pharmaceutical research as potential drug formulations.[9,23,24] As a model system, we tried to prepare PILs from papaverine using different types of natural organic acids, namely citric acid, malic acid, and tartaric acid (α-hydroxy acids, AHAs), succinic acid (carboxylic acid), and meconic acid (β-hydroxy acid). The PILs were compared with papaverine's free base. Papaverine is marketed as chloride salt and used for the treatment of visceral spasms. In order to understand the pattern of the various PILs, they were characterized by means of $^1H-^{15}N$ heteronuclear multiple-bond correlation (HMBC) nuclear magnetic resonance (NMR), X-ray powder diffraction (XRPD), differential scanning calorimetry (DSC), and photometrical dissolution rate measurements. The supramolecular behavior of the papaverine citrate solutions was characterized by means of photometrical and potentiometric solubility measurements, as well as the solubility after 0.5 h and subsequent high-performance liquid chromatography (HPLC) measurements, NMR aggregation assay, viscosity measurements, dynamic light scattering (DLS), and zeta potential measurements.

RESULTS AND DISCUSSION

Structure and Physical Characteristics. The naturally occurring molecule papaverine, a basic secondary metabolite, and a collection of natural organic acids were combined to improve pharmaceutical parameters of the basic alkaloid by the bioinspired strategy of salt formation (Figure 1). As the first step, we prepared various combinations of papaverine and organic acids in different ratios (Table 1).

Table 1. List of Prepared Natural PILs, Protic OILs, and Crystalline Salts

combination	molar ratio	abbreviation
papaverine/citric acid	1:1, 1:2, 1:3	PA 1:1, PA 1:2, PA 1:3
papaverine/succinic acid	1:1	
papaverine/malic acid	1:1, 1:2, 1:3	
papaverine/tartaric acid	1:1, 1:2, 1:3	
papaverine/meconic acid	1:1	

The obtained salts were characterized in their solid state (XRPD, DSC, and dissolution rate) as well as in solution by $^1H-^{15}N$ HMBC NMR measurements as well as ^1H NMR, DLS, zeta potential, solubility, and viscosity to study the supramolecular behavior.

2D NMR Measurements and Solid-State Characterization. The ionic nature of the samples was analyzed by $^1H-^{15}N$ HMBC NMR measurements. In all cases [molar ratio 1:1, 1:2, 1:3, papaverine/organic acid (*i.e.*, citric acid, malic acid, and tartaric acid)], the nitrogen signal of the papaverine was substantially shifted upon protonation; the free base (black) resonated at −79.5 ppm, whereas the nitrogen signal of the hydrochloride (red) resonated at −182.5 ppm, indicating the formation of a salt (Figure 2a). The ^{15}N signals of the citrate were even more shifted, and the nitrogen signal for the 1:1 (black) and 1:3 (red) papaverine citrate occurs at −190 and −192.5 ppm, respectively, indicating a full protonation of the papaverine nitrogen in these mixtures (Figure 2b).

The solid-state forms of the samples were analyzed by means of XRPD (Figure 3). As can be seen from the unstructured diffractograms, papaverine citrate, papaverine malate, and papaverine tartrate [molar ratio 1:1 (PILs), 1:2, 1:3 (protic OILs)] were amorphous salts with decreased crystal lattice energy.[14] This can be explained by intramolecular hydrogen bonding between the hydroxylic group and the free carboxylic acid group present in all AHAs, which diminishes intermolecular interactions between the heterodimers, consisting of

https://dx.doi.org/10.1021/acsomega.0c02630
ACS Omega 2020, 5, 19202−19209

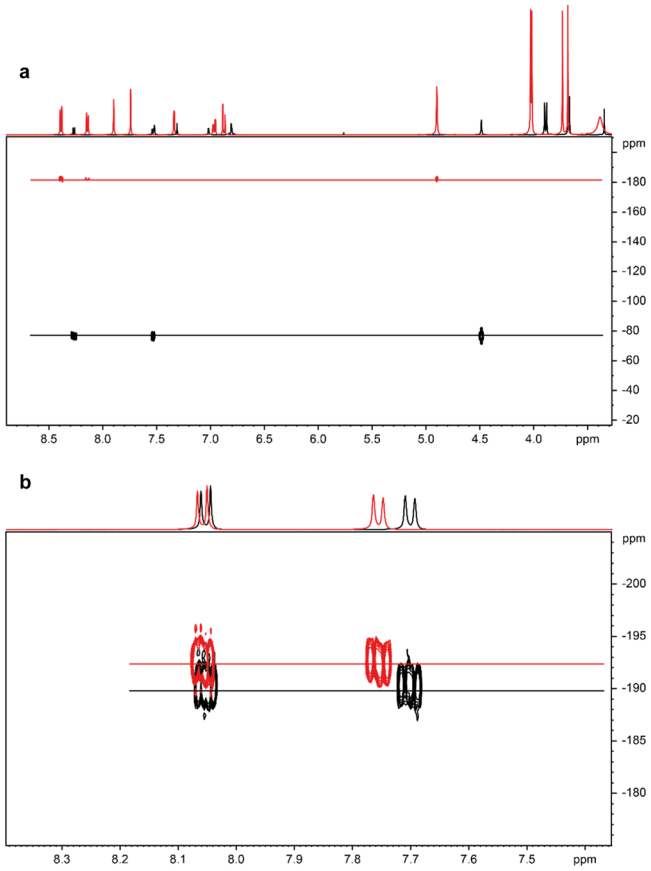

Figure 2. (a) $^{1}H-^{15}N$ NMR spectra of papaverine-free base (black) at −79.5 ppm and papaverine HCl (red) at −182.5 ppm (DMSO-d_6, 5 Hz) and of (b) papaverine/citric acid (molar ratio 1:1, black) at −190 ppm and papaverine/citric acid (molar ratio 1:3, red) at −192.5 ppm (D_2O/KCl, 5 Hz).

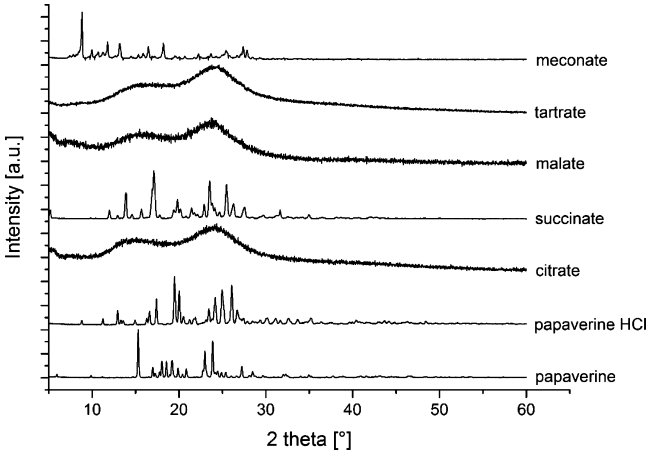

Figure 3. XRPD diffractograms of the papaverine-free base compared to the chloride, citrate, succinate, malate, tartrate, and meconate salts (molar ratio 1:1).

papaverine and AHAs, and thus prevents a long-range molecular order within the solids. In contrast, the papaverine-free base homodimers as well as the heterodimers of papaverine hydrochloride, papaverine succinate, and papaverine meconate were arranged with a certain long-range molecular order because no intramolecular hydrogen bonding was possible within the counterions.[25,26]

The thermal properties of the samples were measured by DSC (Table 2). As expected, all amorphous samples being the

Table 2. DSC Measurement Results of the Samples (Molar Ratio 1:1)

samples	mp [°C]	T_g [°C]
Papaverine	149	
papaverine hydrochloride	220	
papaverine citrate		30
papaverine succinate	134	
papaverine malate		50
papaverine tartrate		40
papaverine meconate	88	

citrate, malate, and tartrate were characterized by a glass transition temperature (T_g) ranging between 30 and 50 °C, whereas the crystalline samples showed a specific mp between 88 and 220 °C with the hydrochloride having by far the highest mp.

Dissolution Rate, Solubility, and Supramolecular Aggregates. The drug substance dissolution rate was measured in phosphate buffered saline (PBS) buffer, pH 6.8. The dissolution rate of the amorphous salts was more than 3-fold higher than the dissolution rate of crystalline salts (Figure 4). The peak concentration during the supersaturation phase

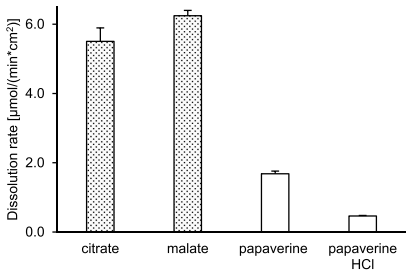

Figure 4. Dissolution rate of the PILs (molar ratio 1:1). Filled bars are amorphous salts, and white bars are crystalline.

(apparent solubility), determined by potentiometric titration in potassium chloride solution, was higher for all amorphous samples (independent of molar ratio). For both groups, the intrinsic solubility (equilibrium solubility) was generally 1 order of magnitude lower than the apparent solubility (Figure 5). Interestingly, both water solubilities, apparent and intrinsic, of papaverine increased with an increasing amount of counterion, which is in accordance with the observation for the drug substance selurampanel (BGG) by Balk.[8] This indicated an intermolecular interaction and stabilization between papaverine and carboxylates, like citrate, malate, or tartrate, which were acting as peptizers.

The supramolecular association of papaverine and the counterion in solution was analyzed by a ^{1}H NMR-based aggregation assay (Figure 6).[27,28] As reference spectra for the lowest aggregation concentration of papaverine, a mixture of papaverine/citric acid (20 mM) and Tween 80 and a solution of papaverine HCl and Tween 80 were prepared. Upon increasing the starting concentration of 20−80 mM of papaverine/citric acid, the signals of the very slightly aggregated papaverine (20 mM) were shifted to the upfield (*e.g.*, 8.2−8.15 or 7.93−7.75 ppm). The concentration-dependent changes in chemical shifts (Δ ppm) can be

https://dx.doi.org/10.1021/acsomega.0c02630
ACS Omega 2020, 5, 19202−19209

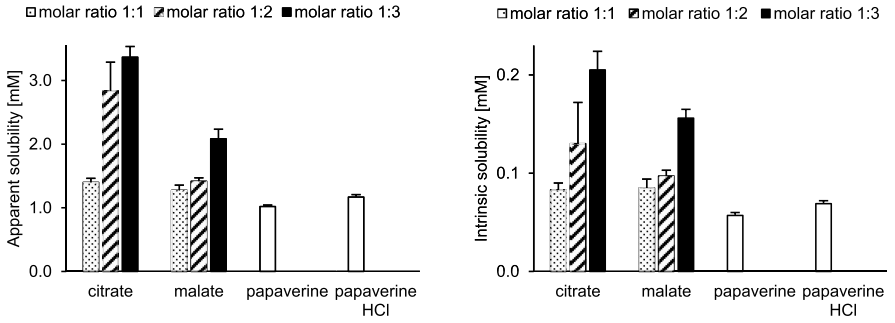

Figure 5. (left) Apparent solubility [mM] and (right) intrinsic solubility [mM] of PILs (different molar ratios), free base, and HCl salt.

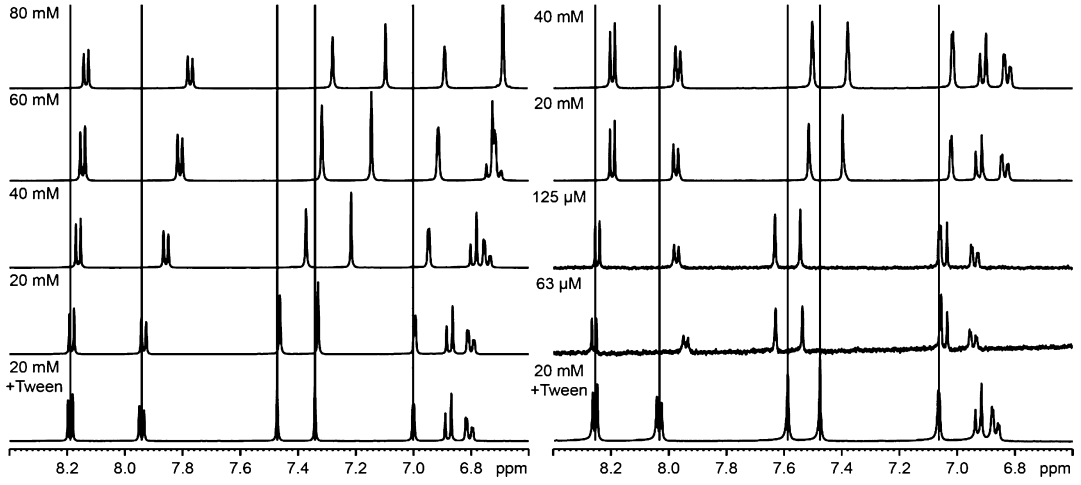

Figure 6. (left) ^{1}H NMR of papaverine citrate (molar ratio 1:1) and (right) of the HCl salt in various concentrations.

Table 3. DLS of Papaverine/Citric Acid (Molar Ratio 1:1, 1:2, 1:3) Compared with Papaverine HCl in Different Papaverine Concentrations in Water

samples	20 mM hydrodynamic diameter [nm]	PDI	40 mM hydrodynamic diameter [nm]	PDI	80 mM hydrodynamic diameter [nm]	PDI
P. HCl	64 ± 69	0.56	38 ± 11	0.24		
	297 ± 113		295 ± 5			
PA 1:1	11 ± 1	0.22	1 ± 0	0.16	2 ± 0	0.20
	254 ± 8		249 ± 5		298 ± 49	
PA 1:2	12 ± 1	0.22	3 ± 2	0.17	3 ± 2	0.20
	301 ± 17		293 ± 16		372 ± 63	
PA 1:3	3 ± 0	0.42	7 ± 7	0.18	12 ± 10	0.17
	959 ± 59		265 ± 17		263 ± 4	

explained by local environmental changes in the magnetic field around the molecule because of the accumulation of aromatic systems with their shielding effects. Another indicator of aggregates is the change in the number of signals, as can be seen at 6.8−6.9 ppm (20 mM) compared with 6.7 ppm (80 mM). The shape of the signal (*i.e.*, sharp or broad) is related to the size and tumbling rate of a supramolecular species. A multimeric species would be expected to have a slower tumbling rate and faster relaxation time and thus a broader peak shape. The broadening of a resonance at higher concentrations is also an evidence for the existence of aggregates. In the ^{1}H NMR spectrum of the papaverine HCl salt, the aromatic signals of papaverine were also shifted to the upfield, indicating aggregation. In contrast to the citrate salt, maximal aggregation is obtained at 20 mM for the hydrochloric acid salt. Moreover, in the 40 mM concentration, precipitation and subsequent sedimentation occurred, which shows the better water solubility of the citrate salt.

The particle size and the polydispersity index (PDI) of supramolecular aggregates of papaverine in water were checked by means of DLS (Table 3). The low PDI < 0.1 indicates monodisperse systems, PDI = 0.1−0.2 refers to a small distribution, and PDI > 0.2 refers to polydisperse systems. It was not possible to measure the 80 mM HCl salt solution because a sedimentation of nondissolved papaverine was observed.

Citric acid performed as the peptizer and stabilized higher concentrations of papaverine (80 mM) with only a small distribution of particle size (PDI about 0.20). Chloride, on the other hand, was not able to stabilize aqueous papaverine solutions in higher concentrations (80 mM) and led to polydisperse solutions (PDI = 0.56) at lower concentrations (20 mM).

The influence of the size of the aggregates with regard to the water solubility of papaverine was investigated (Figure 7). First, the starting concentration (300 mM) of dissolved

https://dx.doi.org/10.1021/acsomega.0c02630
ACS Omega 2020, 5, 19202−19209

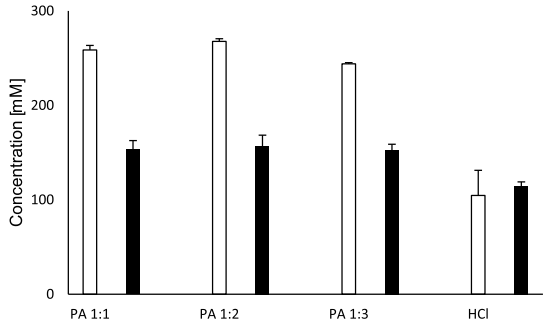

Figure 7. Equilibrium solubility. White bars are unfiltered solutions, and the black bars are filtered solutions.

papaverine in water (PA 1:1, PA 1:2, and PA 1:3) and the supernatant of the papaverine HCl solution were measured by means of HPLC. Second, all solutions were filtered (cellulose acetate filter, pore size 200 nm) to remove all aggregates (>200 nm), and again, the papaverine concentration was determined by HPLC. The concentration of dissolved papaverine decreased significantly for the PILs while no change in the solubility of the HCl salt could be observed. This finding supports the hypothesis of citric acid stabilized and larger supramolecular aggregates of papaverine in accordance with the ^{1}H NMR assay. Chloride as a counterion could not act as a stabilizer for large supramolecular aggregates of papaverine, which led to smaller particles and hence less-dissolved papaverine.

Surface charge properties of nanosuspensions were studied by the measurement of the zeta potential, which is a stability indicating the parameter in colloidal systems. A minimum zeta potential of ±30 mV is required for electrostatically stabilized suspensions. For a combined electrostatic and steric stabilization, roughly ±20 mV is sufficient.[29] The nanosuspensions consisting of papaverine and different concentrations of citric acid were electrostatically stabilized through negatively charged citrate, which is adsorbed on papaverine's surface. This leads to a negative surface of the particles, and through unadsorbed negatively charged citrate in solution, an increased ionic strength results.[25,30] Furthermore, intramolecular hydrogen bonds between the hydroxylic group and the free carboxylic acid group are present in all citric acid ionic species, which hinder attractive particle interactions, leading to a sterically stabilized suspension.[31]

The zeta potential values are commonly calculated by determining particle's electrophoretic mobility in an electric field and then converting the electrophoretic mobility to the zeta potential.[29] This analysis was performed in potassium chloride solution (0.15 M), and the results can be seen as an indicator of long-term stability of the suspension. For the formulation "PA 1:1", a zeta potential of −22 mV was measured, for "PA 1:2" −63 mV, and for "PA 1:3" −5 mV. The largest value of −63 mV indicates the physically most stable suspension while lower values indicate physically instable suspensions. The papaverine hydrochloride salt had a zeta potential of +18 mV. The change of the charge of the aggregates from positive (hydrochloride) to negative (citrate salts) supports the hypothesis of an adsorption of the negatively charged citrate onto the papaverine.

Suspension's viscosity increased with increasing concentration of the counterion (Table 4). The presence of large amounts of unadsorbed negatively charged citrate remaining in solution led to an increased ionic strength and consequently to a decreased Debye length between papaverine aggregates and unadsorbed citrate.[25] The citrate papaverine suspensions offered an increased viscosity compared to the papaverine hydrochloride suspension. This is explained by the nature of the sterically sophisticated citrate in contrast to the small size of chloride as a counterion.

Table 4. Dynamic Viscosity Measurements of Papaverine/Citric Acid (Molar Ratio 1:1, 1:2, 1:3) Compared with Papaverine HCl (40 mM Papaverine)

samples	dynamic viscosity [mPa s]
water	0.88
KCl solution	0.88
papaverine HCl (in KCl)	0.93
PA 1:1 (in water)	0.94
PA 1:2 (in water)	0.95
PA 1:3 (in water)	0.97

CONCLUSIONS

Taking everything into consideration, organic acids acting as counterions for basic secondary metabolites and facilitate the formation of PILs and protic OILs. The beneficial properties of these salts consisting of APIs and naturally occurring organic acids, like enhanced dissolution rate, increased apparent solubility, and stabilized suspensions, offer a promising strategy to optimize pharmaceutical parameters. Also, the low acquisition costs and the safety of most naturally occurring organic acids are promising for novel pharmaceutical salts and clinical translation thereof. In the future, we will perform further salt screening programs with natural organic acids in order to demonstrate the applicability of the bioinspired approach, and the obtained PILs herein will be analyzed in terms of enhanced solubility studies *in vitro* and *in vivo* as well as the membrane transport.

EXPERIMENTAL SECTION

Materials. Papaverine was purchased from Fagron GmbH & Co. KG (Barsbüttel, Germany). Citric acid, succinic acid, malic acid, and tartaric acid were purchased from Sigma-Aldrich (Schnelldorf, Germany) or TCI Chemicals (Eschborn, Germany) and were used without further purification. Meconic acid was synthesized following the literature.[32] Ultrapure water was delivered by the Merck Milli-Q system (Darmstadt, Germany).

Methods. *Preparation of PILs, Protic OILs, and Low-Melting Salts.* PILs, protic OILs, and low-melting papaverine salts were prepared in analogy to previous reports.[33] Briefly, 100 mg of papaverine was suspended in 5 mL of methanol and an equimolar amount (2-fold or 3-fold excess, respectively) of the counterion (organic acid) suspended in 5 mL of methanol was added and mixed for 15 min at room temperature. Solvents were evaporated under ambient conditions for 3 days and subsequently dried *in vacuo*.

NMR Measurement. NMR measurement was performed on a Bruker Avance III 400 MHz spectrometer (Karlsruhe, Germany) operating at 400.13 MHz with a PA BBI inverse probe head, and data were processed with the TopSpin 3.5pl7 software.

For ^{1}H NMR, the acquisition parameters were applied as follows: 16 scans, at a temperature of 300 K, flip angle of 30°, spectral width of 20.55 ppm, and transmitter offset of 6.175

https://dx.doi.org/10.1021/acsomega.0c02630
ACS Omega 2020, 5, 19202−19209

ppm. The acquisition time was set to 3.985 s followed by a relaxation delay of 1.0 s with a collection of 64k data points at a sample spinning frequency of 20 Hz. Processing parameters were set to an exponential line broadening window function of 0.3 Hz, an automatic baseline correction, and manual phasing. After a setting time of 5 min at 300 K, the spectra were recorded in D_2O.

The 2D $^{1}H-^{15}N$ HMBC spectra were recorded at 300 K with 128 increments in t_1. The long-range coupling constant was set to 5 Hz. The data were processed using a sine window function in both dimensions, zero-filling in the F_1 dimension and linear prediction in the t_1 dimension prior to Fourier transformation. Automatic baseline correction in both dimensions was performed.

X-ray Powder Diffractometry. PILs, protic OILs, and crystalline papaverine salts were transferred onto a silicon single-crystal zero background specimen holder, covering an area with the diameter of approximately 5 mm. Powder diffractometric studies were done using a Bruker Discover D8 powder diffractometer (Karlsruhe, Germany) and Cu Kα radiation (unsplit Kα_1 + Kα_2 doublet, mean wavelength l = 154.19 pm) at a power of 40 kV and 40 mA, a focusing Goebel mirror, and a 2.5° axial Soller slit. The scattered X-ray beam went through a receiving slit (3.3°). Detection was done with a LynxEye-1D detector (Bruker AXS) using the full detector range of 192 channels. Measurements were carried out in the reflection geometry in coupled $2\theta/\theta$ mode with a step size of 0.025° in 2θ and 0.33 s measurement time per step in the range of 5−50° (2θ). Data collection was done with the software package DIFFRAC.Suite (V2 2.2.690, Bruker AXS, Karlsruhe, Germany). The diffraction data were subsequently converted into the ASCII format and further handled with Origin (OriginLab, Massachusetts, USA).

Photometrical Determination of the Dissolution Rate. Dissolution rates were measured with a Sirius T3 instrument (Sirius Analytical, Forest Row, UK) as described earlier.[34] Tablets with defined surfaces were prepared by compression of 5−10 mg of substance (salt or papaverine-free base) in a tablet disk (diameter of the tablet disk was 0.3 cm and is provided by the manufacturer of the machine) under a weight of 0.18 tonnes for 3 min with a manual hydraulic tablet press (Paul Weber, Stuttgart, Germany), as described before.[34] The release of drug substance from these tablet disc allows data collection with a standardized surface area (0.07 cm^2), which is required to fit the data for the calculation of the dissolution rate.[34] The dissolution rates were determined photometrically at room temperature in PBS (0.17 M) pH 6.8 at a stirring speed of 4800 rpm following manufacturer's instructions. The linear part of the release profile was used for calculation of the dissolution rate (dissolved substance per time and surface area).

Potentiometrically and Photometrically Recorded Titration Experiments for Determination of Solubility. Intrinsic and apparent solubility were measured on a Sirius T3 instrument (Sirius Analytical, Forest Row, UK) by potentiometric titration as described before.[35,36] In brief, typically 5−10 mg of API was dissolved in 1.5 mL of 0.15 M KCl solution at pH 2 (adjusted with 0.5 M hydrochloric acid). After complete dissolution, the solution was back-titrated by addition of 0.5 M potassium hydroxide until first precipitation occurred and as continuously monitored photometrically (λ = 500 nm). Subsequently, the pH was changed incrementally by repeated addition of minute amounts of acid and base throughout the experiment. After each titrant addition, the delayed pH gradient of the API because of precipitation or dissolution was measured and used to extrapolate the equilibrium phase where the gradient is zero. Data from analysis with acidity errors larger than 1 mM were excluded.

Differential Scanning Calorimetry. DSC was performed on a DSC 8000 instrument (PerkinElmer, Waltham, MA, USA) using a scanning rate of 20 K/min. The sample size was 3−5 mg for all substances. For the PILs, three heating and three cooling cycles were performed, and the second and the third heating cycles were analyzed to allow for removal of residual water during the first heating cycle. Crucibles were weighted before and after measurements.

DLS Sample Preparation and Analysis. The average particle size of different concentrations of papaverine citrate and papaverine hydrochloric acid salt (20, 40, 80 mM) in water was measured by DLS. Measurements were performed with unfiltered samples in disposable UV-cuvettes (1.5 mL) from Brand (Wertheim, Germany) using a Delsa Nano HC particle analyzer from Beckman Coulter (Brea, CA, USA) with backscattering at an angle of 165°. Measurements were performed in triplicate with an accumulation of 70 scans at 298 K, and the data were analyzed by the CONTIN algorithm. The average particle sizes were evaluated with a refractive index of 1.333 for all samples, and the experimentally measured dynamic viscosities of the specific solutions were also used (see also Determination of Dynamic Viscosity).

Zeta Potential Measurement. Zeta potential measurements of the papaverine salts (40 mM) in potassium chloride solution (0.15 M) were performed in deionized water with its conductivity adjusted to 50 $\mu S/cm^2$, in order to determine the surface charge and to estimate the long-term stability properties. The analysis was performed by using a Delsa Nano HC particle analyzer from Beckman Coulter (Brea, CA, USA) at 298 K with a flow cell (60 V, base frequency 115−140 Hz, scattering angle 15°). The electrophoretic mobility was converted to the zeta potential by the Helmholtz−Smoluchowski equation. All measurements were performed in triplicate.

Liquid Chromatography. All HPLC analyses were performed with an Agilent 1100 modular chromatographic system equipped with an online vacuum degasser, a binary pump, an autosampler, a thermostatted column compartment, and a variable wavelength detector (Agilent, Waldbronn, Germany). The system was operated, and the data were processed using the Agilent ChemStation Rev. B.03.02. software.

A Hypersil GOLD C18 column (150 × 4.6 mm i.d., with a particle size of 5 μm and a pore size of 100 Å) (Thermo Fisher Scientific, Waltham, MA, USA) was used as a stationary phase. Mobile phase A consisted of an aqueous 10 mM dipotassium hydrogen phosphate buffer adjusted to pH 7.4 with orthophosphoric acid while mobile phase B was methanol. The gradient worked at a flow rate of 1.0 mL/min and utilized a linear gradient from 10 to 90% B from 0 to 25 min. 90% B is then hold isocratically for 5 min, and the system is reequilibrated by a gradient back to 10% within 2 min followed by a 3 min isocratic step. The total run time was 35 min, and the injection volume was 10 μL. The UV detection was performed at 254 nm, and the runs were recorded at ambient temperature.

Determination of Dynamic Viscosity. The density was determined using Anton Paar (Graz, Austria) density meter

https://dx.doi.org/10.1021/acsomega.0c02630
ACS Omega 2020, 5, 19202−19209

DMA 4100 M at 298 K. The dynamic viscosity was measured on Anton Paar (Graz, Austria) rolling-ball viscometer LOVIS 2000 M using capillary LOVIS 1.8 equipped with a steel ball (Mat. no. 73109, diameter 1.5 mm, steel 1.4125, density 7.66 g/cm^3). The temperature was constantly maintained at 298 K, and the inclination angle was 70° for all measurements.

AUTHOR INFORMATION

Corresponding Author

Ulrike Holzgrabe − *Institute of Pharmacy and Food Chemistry, University of Würzburg, DE-97074 Würzburg, Germany;* orcid.org/0000-0002-0364-7278; Email: ulrike.holzgrabe@uni-wuerzburg.de

Authors

Paul Güntzel − *Institute of Pharmacy and Food Chemistry, University of Würzburg, DE-97074 Würzburg, Germany*

Klaus Schilling − *Institute of Pharmacy and Food Chemistry, University of Würzburg, DE-97074 Würzburg, Germany*

Simon Hanio − *Institute of Pharmacy and Food Chemistry, University of Würzburg, DE-97074 Würzburg, Germany;* orcid.org/0000-0003-4624-8020

Jonas Schlauersbach − *Institute of Pharmacy and Food Chemistry, University of Würzburg, DE-97074 Würzburg, Germany;* orcid.org/0000-0002-3746-3004

Curd Schollmayer − *Institute of Pharmacy and Food Chemistry, University of Würzburg, DE-97074 Würzburg, Germany*

Lorenz Meinel − *Institute of Pharmacy and Food Chemistry, University of Würzburg, DE-97074 Würzburg, Germany;* orcid.org/0000-0002-7549-7627

Complete contact information is available at: https://pubs.acs.org/10.1021/acsomega.0c02630

Funding

This publication was supported by the Open Access Publication Fund of the University of Würzburg.

Notes

The authors declare no competing financial interest.

ACKNOWLEDGMENTS

Our thanks go out to Dr. Johannes Wiest for his support and advice during the whole project.

REFERENCES

(1) Farré, E. M.; Tiessen, A.; Roessner, U.; Geigenberger, P.; Trethewey, R. N.; Willmitzer, L. Analysis of the compartmentation of glycolytic intermediates, nucleotides, sugars, organic acids, amino acids, and sugar alcohols in potato tubers using a nonaqueous fractionation method. *Plant Physiol.* **2001**, *127*, 685−700.

(2) Martinoia, E.; Massonneau, A.; Frangne, N. Transport processes of solutes across the vacuolar membrane of higher plants. *Plant Cell Physiol.* **2000**, *41*, 1175−1186.

(3) Frei, B.; Eisenach, C.; Martinoia, E.; Hussein, S.; Chen, X.-Z.; Arrivault, S.; Neuhaus, H. E. Purification and functional characterization of the vacuolar malate transporter tDT from Arabidopsis. *J. Biol. Chem.* **2018**, *293*, 4180−4190.

(4) Neuhaus, H. E. Transport of primary metabolites across the plant vacuolar membrane. *FEBS Lett.* **2007**, *581*, 2223−2226.

(5) Hamilton, G. R.; Baskett, T. F. In the arms of morpheus: the development of morphine for postoperative pain relief. *Can. J. Anaesth.* **2000**, *47*, 367−374.

(6) Sertürner, F. W. Trommsdorff's Journal der Pharmazie für Aerzte. *Apotheker und Chemisten* **1805**, *13*, 229−235.

(7) Domingos, S.; André, V.; Quaresma, S.; Martins, I. C. B.; Minas da Piedade, M. F.; Duarte, M. T. New forms of old drugs: improving without changing. *J. Pharm. Pharmacol.* **2015**, *67*, 830−846.

(8) Balk, A.; Widmer, T.; Wiest, J.; Bruhn, H.; Rybak, J.-C.; Matthes, P.; Müller-Buschbaum, K.; Sakalis, A.; Lühmann, T.; Berghausen, J.; Holzgrabe, U.; Galli, B.; Meinel, L. Ionic liquid versus prodrug strategy to address formulation challenges. *Pharm. Res.* **2015**, *32*, 2154−2167.

(9) Marrucho, I. M.; Branco, L. C.; Rebelo, L. P. N. Ionic liquids in pharmaceutical applications. *Annu. Rev. Chem. Biomol. Eng.* **2014**, *5*, 527−546.

(10) Welton, T. Room-Temperature Ionic Liquids. Solvents for Synthesis and Catalysis. *Chem. Rev.* **1999**, *99*, 2071−2084.

(11) Ferraz, R.; Branco, L. C.; Prudêncio, C.; Noronha, J. P.; Petrovski, Ž. Ionic liquids as active pharmaceutical ingredients. *ChemMedChem* **2011**, *6*, 975−985.

(12) Easton, M. E.; Choudhary, H.; Rogers, R. D. Azolate Anions in Ionic Liquids: Promising and Under-Utilized Components of the Ionic Liquid Toolbox. *Chem.—Eur. J.* **2019**, *25*, 2127−2140.

(13) Fukaya, Y.; Iizuka, Y.; Sekikawa, K.; Ohno, H. Bio ionic liquids: room temperature ionic liquids composed wholly of biomaterials. *Green Chem.* **2007**, *9*, 1155−1157.

(14) Agharkar, S.; Lindenbaum, S.; Higuchi, T. Enhancement of Solubility of Drug Salts by Hydrophilic Counterions: Properties of Organic Salts of an Antimalarial Drug. *J. Pharm. Sci.* **1976**, *65*, 747−749.

(15) Balk, A.; Holzgrabe, U.; Meinel, L. Pro et contra ionic liquid drugs—Challenges and opportunities for pharmaceutical translation. *Eur. J. Pharm. Biopharm.* **2015**, *94*, 291−304.

(16) Stoimenovski, J.; Dean, P. M.; Izgorodina, E. I.; MacFarlane, D. R. Protic pharmaceuticalionic liquids and solids: Aspects of protonics. *Faraday Discuss.* **2012**, *154*, 335−352.

(17) Easton, M. E.; Li, K.; Titi, H. M.; Kelley, S. P.; Rogers, R. D. Controlling the Interface between Salts, Solvates, Co-crystals, and Ionic Liquids with Non-stoichiometric Protic Azolium Azolates. *Cryst. Growth Des.* **2020**, *20*, 2608−2616.

(18) Greaves, T. L.; Drummond, C. J. Protic Ionic Liquids: Evolving Structure-Property Relationships and Expanding Applications. *Chem. Rev.* **2015**, *115*, 11379−11448.

(19) Johansson, K. M.; Izgorodina, E. I.; Forsyth, M.; MacFarlane, D. R.; Seddon, K. R. Protic ionic liquids based on the dimeric and oligomeric anions: $[(AcO)_xH_{x-1}]^-$. *Phys. Chem. Chem. Phys.* **2008**, *10*, 2972−2978.

(20) Bica, K.; Rogers, R. D. Confused ionic liquid ions-a "liquification" and dosage strategy for pharmaceutically active salts. *Chem. Commun.* **2010**, *46*, 1215−1217.

(21) Samin, S.; Hod, M.; Melamed, E.; Gottlieb, M.; Tsori, Y. Experimental Demonstration of the Stabilization of Colloids by Addition of Salt. *Phys. Rev. Appl.* **2014**, *2*, 024008.

(22) Israelachvili, J. *Intermolecular and Surface forces*, 3rd ed.; Academic Press: London, U.K., 2011.

(23) Egorova, K. S.; Gordeev, E. G.; Ananikov, V. P. Biological Activity of Ionic Liquids and Their Application in Pharmaceutics and Medicine. *Chem. Rev.* **2017**, *117*, 7132−7189.

(24) Shamshina, J. L.; Barber, P. S.; Rogers, R. D. Ionic liquids in drug delivery. *Expert Opin. Drug Delivery* **2013**, *10*, 1367−1381.

(25) Hidber, P. C.; Graule, T. J.; Gauckler, L. J. Citric Acid-A Dispersant for Aqueous Alumina Suspensions. *J. Am. Ceram. Soc.* **1996**, *79*, 1857−1867.

(26) Dengale, S. J.; Grohganz, H.; Rades, T.; Löbmann, K. Recent advances in co-amorphous drug formulations. *Adv. Drug Delivery Rev.* **2016**, *100*, 116−125.

(27) LaPlante, S. R.; Carson, R.; Gillard, J.; Aubry, N.; Coulombe, R.; Bordeleau, S.; Bonneau, P.; Little, M.; O'Meara, J.; Beaulieu, P. L. Compound aggregation in drug discovery: implementing a practical NMR assay for medicinal chemists. *J. Med. Chem.* **2013**, *56*, 5142−5150.

(28) Wiest, J.; Saedtler, M.; Böttcher, B.; Grüne, M.; Reggane, M.; Galli, B.; Holzgrabe, U.; Meinel, L. Geometrical and Structural

Dynamics of Imatinib within Biorelevant Colloids. *Mol. Pharm.* **2018**, *15*, 4470−4480.
(29) Jacobs, C.; Müller, R. H. Production and characterization of a budesonide nanosuspension for pulmonary administration. *Pharm. Res.* **2002**, *19*, 189−194.
(30) Araújo, F. A.; Kelmann, R. G.; Araújo, B. V.; Finatto, R. B.; Teixeira, H. F.; Koester, L. S. Development and characterization of parenteral nanoemulsions containing thalidomide. *Eur. J. Pharm. Sci.* **2011**, *42*, 238−245.
(31) Leong, Y.-K. Role of Molecular Architecture of Citric and Related Polyacids on the Yield Stress of α-Alumina Slurries: Inter- and Intramolecular Forces. *J. Am. Ceram. Soc.* **2010**, *93*, 2598−2605.
(32) Güntzel, P.; Forster, L.; Schollmayer, C.; Holzgrabe, U. A Convenient Preparation of Carboxy-γ-pyrone Derivatives: Meconic Acid and Comenic Acid. *Org. Prep. Proced. Int.* **2019**, *50*, 512−516.
(33) Bica, K.; Rijksen, C.; Nieuwenhuyzen, M.; Rogers, R. D. In search of pure liquid salt forms of aspirin: ionic liquid approaches with acetylsalicylic acid and salicylic acid. *Phys. Chem. Chem. Phys.* **2010**, *12*, 2011−2017.
(34) Gravestock, T.; Box, K.; Comer, J.; Frake, E.; Judge, S.; Ruiz, R. The "GI dissolution" method: a low volume, in vitro apparatus for assessing the dissolution/precipitation behaviour of an active pharmaceutical ingredient under biorelevant conditions. *Anal. Methods* **2011**, *3*, 560.
(35) Hsieh, Y.-L.; Ilevbare, G. A.; Van Eerdenbrugh, B.; Box, K. J.; Sanchez-Felix, M. V.; Taylor, L. S. pH-Induced precipitation behavior of weakly basic compounds: determination of extent and duration of supersaturation using potentiometric titration and correlation to solid state properties. *Pharm. Res.* **2012**, *29*, 2738−2753.
(36) Stuart, M.; Box, K. Chasing equilibrium: measuring the intrinsic solubility of weak acids and bases. *Anal. Chem.* **2005**, *77*, 983−990.

https://dx.doi.org/10.1021/acsomega.0c02630
ACS Omega 2020, 5, 19202−19209